MULTIDIMENSIONAL WAVELET ANALYSIS FOR RECOGNITION OF LESIONS IN COLPOSCOPY TEST

Diana Ivone Tapia López, Aldrin Barreto Flores and Leopoldo Altamirano Robles

National Institute of Astrophysics, Optics and Electronics, Computer Science Department
Luis Enrique Erro No.1, Sta. María Tonantzintla, 72840, Puebla, México

Keywords: Cervical cancer, temporal texture analysis, wavelet analysis, wavelet-aggregated signal.

Abstract: Cervical cancer is an important worldwide disease due the high rate of incidence in the population. Colposcopy is one of the diagnostic tests employed in recognition of lesions, which performs a visual examination of the cervix based on temporal reaction of the surface stained with acetic acid. It is proposed in this paper to evaluate the temporal texture changes produced by the acetic acid based on the concept of the wavelet-aggregated signal in order to identify lesions. An aggregated signal is a scalar signal providing maximum information on the most general variations present in all the processes analyzed and at the same time suppressing components that are characteristic of individual processes. Texture metrics based on spatial information are used in order to analyze temporally the acetic acid response and deduce appropriate signatures. Later, temporal information is analyzed using multidimensional wavelet analysis for identification of lesions.

1 INTRODUCTION

An important disease that has been widely studied is the cervical cancer due the high rate of incidence in the population. Actually, a group of tests have been developed for the early diagnosis of this illness: Pap smear, colposcopy and biopsy (Claude, Winzenrieth, et al, 2002). Colposcopy test evaluates several reactions appearing after the application of acetic acid on the surface of the cervix; it makes a visual analysis of the cervix surface using a large microscope called colposcope, finding lesions and observing their severity (Parker, Karins and O'Connor, 1998). The acid causes the appearance or emphasis of lesions visually analyzed by the physician (Burghardt, 1991). Several computer vision based solutions have been proposed in order to automatically identify abnormalities in the cervix using colposcopy images.

An image analysis using pixel intensity is presented in (Pogue, Myceck and Harper, 2000), evaluating the Red-Green-Blue (RGB) channels, spatial frequencies, fractal dimension and Euler number, which was the best criteria for the discrimination of cervical neoplasia using a small set of cases. Different computer vision techniques have

been also used in other works, for example, color and texture analysis using pixel co-ocurrence matrix for segmentation of lesions (Claude, Pouletaut, et al, 2001). A colposcopy images classification using edge features is presented in (Claude, Winzenrieth, et al, 2002). Authors generate a digital signature of 6 contour patterns and analyze the power spectrum of each one, in order to detect discriminatory patterns that are learned in a neural network. Related works, which analyze images to discriminate colposcopy lesions lack of generality because they focus in a single feature of the lesion, reporting a better characterization of the lesions the use of temporal information, as is described in (Parker, Karins and O'Connor, 1998), (Tumer, Ramanujam et al, 1998) and (Parker, Mooradian, et al, 2002).

In this paper we propose to evaluate the temporal texture changes produced by the acetic acid based on the concept of the wavelet-aggregated signal in order to identify lesions in cervix region. Spatial texture metrics are used for analysis of temporal changes on cervix surface. These metrics are based in gray level information between pixels and they are suitable for characterization of lesions in cervix. We show how temporal information of texture analysis can be used to perform multidimensional wavelet analysis, in

order to identify those regions in cervix where lesions are presented.

The rest of this paper is organized as follows: next section presents a briefly description of texture metrics and temporal information obtained*;* in section 3 wavelet-aggregated signal is briefly described; image sequences used in this work are presented in section 4; experimental results are described in section 5; finally, some conclusions and directions for future work are presented in section 6.

2 TEMPORAL TEXTURE METRICS

2.1 Texture Metrics

The analysis of temporal changes on the cervix surface has been performed using the metrics presented in (Baeg, Kehtarnavaz, 2002) to classify breast mass. These metrics are well correlated with colposcopy exam because features of lesions are similar to the breast mass (Tapia, Barreto and Altamirano, 2006).

Denseness measure is obtained by calculating the distribution of gray values, maxima/minima local points in rows and columns. The idea is to produce a binary image that represents the distribution of maxima and minima gray values in a region of interest. A pixel is considered local column maximum and it is assigned a zero value in the binary image if its value in the original image is greater than its neighbors, in other case it is assigned one. The equation (1) shows the calculation of local column maximum and (2) local row maximum.

$$g(x-1,y) < g(x,y) > g(x+1,y) \ . \tag{1}$$

$$g(x,y-1) < g(x,y) > g(x,y+1) \ . \tag{2}$$

Architectural distortion is associated with new details revealed by the acetic acid and it can be quantified using a gradient based measure like in (Baeg, Kehtarnavaz, 2002), because new details appears like small points, mosaics and edges. The equation used for its calculation is presented in (3). The values N_1 and N_2 correspond to the number of pixels in which gradient were different to zero. This process uses just those pixels that are presenting changes in the image. The 3 value in the equation is used in order to increase the presence of changes presented in the image. A small change cannot increase so much while a high change can be more noticeable.

$$I = \frac{\sum_{\forall(x,y)} |g(x,y+1) - g(x,y)|^3}{N_1} + \frac{\sum_{\forall(x,y)} |g(x+1,y) - g(x,y)|^3}{N_2} \ . \tag{3}$$

A detail description of the metrics can be consulted in (Baeg, Kehtarnavaz, 2002).

2.2 Temporal Texture Analysis

Denseness and architectural distortion values are extracted and tracked in each frame of the sequence, selecting a region of interest during the acetic acid reaction. Graphs in Figure 1 show the temporal changes occurring when we select a normal and abnormal region of interest over the cervix surface.

Density presents no significant changes in its temporal behavior for normal cases (lower curve) because the acetic acid is not producing changes in the cervix surface, while in abnormal cases (upper curve) significant changes are represented by a decrease in the slope at the end of the curve.

Architectural distortion evaluation is presented in Fig. 1.b. The abnormal curve presents an increasing slope because new details appear as the cervix surface reacts with the acetic acid, while normal region is not presenting changes. it's important to remark the difference between normal and abnormal cases and how the temporal behavior of metrics can be used for discrimination and identification of lesions in a colposcopy exam using a computer vision approach.
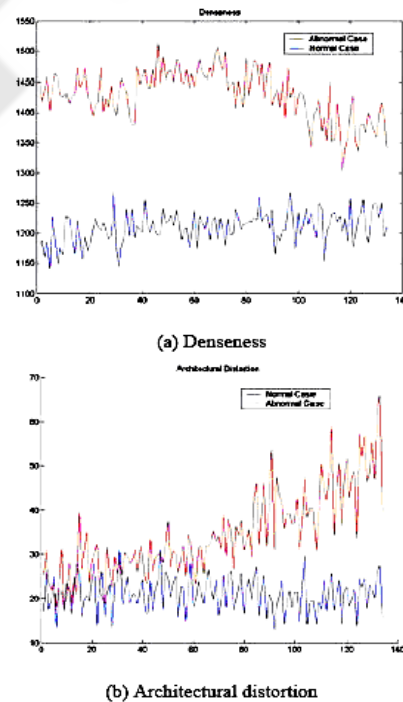

(a) Denseness

(b) Architectural distortion

Figure 1: Temporal texture analysis of medical cases.

3 WAVELET AGGREGATED SIGNAL

The concept of the wavelet-aggregated signal was previously introduced by (Lyubushin, 1998). An aggregated signal is a scalar signal providing maximum information on the most general variations present in all of the processes analyzed and at the same time suppressing components that are characteristic of individual processes and that usually represent local noise. The aggregated signal is constructed in two stages that will be described below. A detailed description of the wavelet-aggregated signal can be found in (Lyubushin, 2000).

Below, only Haar wavelets (4) are used. This choice is dictated by the fact that we seek the most pronounced common variations for which basis (4) is best suited.

$$\Psi(t) = -1 \; if \; t \in \left(0, \frac{1}{2}\right]$$

$$+1 \; if \; t \in \left(\frac{1}{2}, 1\right] \; 0 \; for \; other \; t, \tag{4}$$

Let $x(t)$ be a signal with a discrete time t N samples long, $t = t_j = j\Delta t, j = 1, \ldots, N$. It is assumed that N is an integer of the 2^m type, which is convenient for the subsequent use of the fast wavelet transformation. If N is not equal to 2^m, the signal $x(t)$ can be complemented by zeros until its length becomes 2^m, where m is the minimum integer for which $N \leq 2^m$. In the case of a finite sample and discrete time, the formula for multiresolution analysis is

$$x(t) = d + \sum_{\alpha=1}^{m} x^{(\alpha)}(t),$$

$$x^{(\alpha)}(t) = \sum_{j=1}^{2^{(m-\alpha)}} c^{(\alpha)}(\tau_j^{(\alpha)}) \Psi^{(\alpha)}(t - \tau_j^{(\alpha)}), \tag{5}$$

$$\tau_j^{(\alpha)} = j \; X \; 2^{\alpha} \Delta t.$$

The coefficient d in (5) is equal to the mean of $x(t)$, $t = 1, \ldots, N$. The set of values $c^{(\alpha)}(\tau_j^{(\alpha)})$ and d are calculated using the direct fast wavelet transformation. The wavelet-aggregated signal is constructed in two stages.

The first stage initially involves the calculation of the wavelet coefficients for each time series under study and at each scale level using the fast discrete wavelet transformation. Before the transformation, the time series are converted to series in increments and are normalized in order to provide diverse physical signals of different scales for join processing. The initial wavelet coefficients are then converted to the so-called canonical wavelet coefficients, which are obtained from covariance matrices of wavelet coefficients at each detail level using the method of canonical correlations. This conversion aims at removing individual noise from the wavelet coefficients and to amplify the common component.

At the second stage, the intensity of the common component is additionally increased by calculating the first main component of the covariance matrices of canonical wavelet coefficients at each detail level. Thus, a scalar sequence of hypothetical wavelet coefficients is obtained at each detail level, which makes it possible to calculate the inverse discrete fast wavelet transform and to obtain the time realization of a scalar signal called the wavelet-aggregated signal of the initial time series.

4 COLPOSCOPY IMAGE SEQUENCES

Sequences used in this work include 8 abnormal medical cases shown in Figure 2, captured by a couple of colposcopy specialists in a public health institution in Mexico. The equipment used for the capture was a standard colposcope, a framegrabber and a digital camera. Sequences were acquired after the acetic acid application in order to register the most important changes on the cervix.
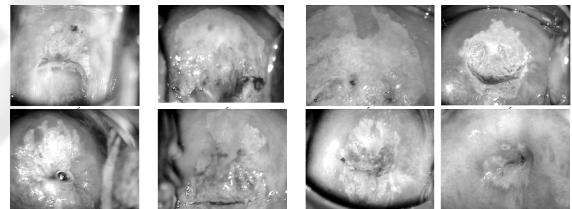

Figure 2: Abnormal medical cases used in the study.

The size of the sequences varies in a range of 160 frames to 240 frames and the capture time is about 8-12 seconds, that is the time that colposcopy test last, using a rate of 20 frames per second. Images in Figure 3 present the initial frame before acetic acid application and the last frame of the sequence after the acetic acid reaction has occurred.

There are some problems that must be solved in order to have a correct temporal analysis: the *image stabilization* and the *non uniform illumination*. A more detailed description of the methods used here is described in (Barreto, Altamirano, 2005).
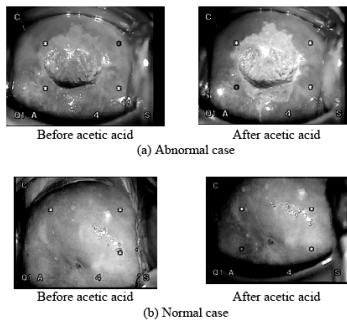
Before acetic acid   After acetic acid
(a) Abnormal case

Before acetic acid   After acetic acid
(b) Normal case

Figure 3: Texture changes after acetic acid application.

5 RESULTS

After image stabilization and non uniform illumination correction processes are performed, texture metrics are applied to the sequences for temporal analysis estimation. After that, results of temporal analysis are processed using the wavelet-aggregated signal to identify lesions in cervix.

We just present results of architectural distortion in this paper because this metric achieved in better results in wavelet analysis. In every abnormal case a region of interest to be analyzed along the sequence was selected. This region was divided in several subregions that were analyzed with texture metrics, and the resulting curve describes the temporal behavior of each subregion. Results of temporal information are presented in Figure 4.

As we can see in Figure 4, in those subregions where new details appear, the curve suffers an increase in its slope value, while values in normal regions do not present important changes, identifying lesions in cervix accurately.

Results obtained from temporal analysis were processed using the wavelet-aggregated signal described previously. It's important to highlight that wavelet analysis allows to identify lesions, eliminating components that are characteristic of individual processes, like local noise caused by measurement uncertainties. The wavelet-aggregated signal for every abnormal case is constructed with the time series described by each subregion in the region of interest. So, we have N time series for every abnormal case to be analyzed in the construction of the wavelet. N is the total amount of subregions in every case.

The method described in section 3 produce a new signal that is characterized by significantly lower noise and preserves the most informative variations in time during the test.

Figure 4 plots the wavelet-aggregated signal for every abnormal case, showing over the horizontal axis the subregion where lesions appear. For a better appreciation of results, we also show standard deviation and mean values in every case, splitting data in normal and abnormal subregions and getting two measures for each case. These measures are summarized in Table 1. It can be noticed that standard deviation value in normal subregions is smaller than those subregions where lesions appeared, showing data dispersion and variations in the signal.

In the same way, the wavelet-aggregated signal generated in every case show variations in those subregions where significant changes are present. This analysis give support to temporal analysis performed with texture metrics.

We can compare graphs for texture metrics with the wavelet-aggregated signal of every abnormal case, in order to identify subregions where lesions appear as for example subregions 9 to 12 and 25 to 26 in the first medical case, where it can be noticed an increase in the slope of the curve and a significant variation in the wavelet obtained in these same regions. The rest of the wavelet signal preserves its normal value, not showing significant variation in the amplitude value.

We also performed classification process using information of wavelet analysis to give support to our method. We use 1-NN, Simple Naive Bayes and Backpropagation as learning algorithms and 10-fold cross validation as test mode. Classification results are shown in Table 2.

Table 1: Mean and standard deviation values for normal and abnormal regions in medical cases.

MC	Normal	Abnormal
1	$\bar{x} = 0.23316$	$\bar{x} = 1.8631$
	$\sigma = 0.83931$	$\sigma = 5.3664$
2	$\bar{x} = 0.17536$	$\bar{x} = 1.365$
	$\sigma = 0.73117$	$\sigma = 4.2666$
3	$\bar{x} = 0.12835$	$\bar{x} = 1.4254$
	$\sigma = 0.72382$	$\sigma = 3.6212$
4	$\bar{x} = 0.1592$	$\bar{x} = 0.062167$
	$\sigma = 0.47121$	$\sigma = 0.84576$
5	$\bar{x} = 0.33906$	$\bar{x} = 0.85605$
	$\sigma = 1.1207$	$\sigma = 2.5982$
6	$\bar{x} = 0.09307$	$\bar{x} = 0.65914$
	$\sigma = 0.53559$	$\sigma = 1.8261$
7	$\bar{x} = 1.8197$	$\bar{x} = 23.619$
	$\sigma = 5.689$	$\sigma = 45.611$
8	$\bar{x} = 0.64328$	$\bar{x} = 5.9494$
	$\sigma = 1.7862$	$\sigma = 17.466$

Can be observed that features used in classification process achieved in good results, even when accuracy in classification is not a high value in some cases. The F-measure is a popular combination of precision and recall into a single parameter, showing that classifications of lesions can be identified with some precision. Although classification gives good results, more features can be used in order to increase accuracy in identification of lesions.

Multidimensional wavelet analysis performed in this work shows how useful is temporal information for identification of lesions in cervix, enhancing our previous work, and giving reliability to our method.

6 CONCLUSIONS

We have presented an approach about identification of lesions in the cervix based on temporal texture analysis. Results show the importance of temporal analysis in identification of lesions and how this information can be used in later analysis, in order to enhance lesions detection process.

Wavelet analysis allows to process data at different scales or resolutions. Main advantage over traditional Fourier methods is that wavelet analyzes physical situations where the signal contains discontinuities and sharp spikes, highlighting abnormalities found in temporal analysis of colposcopy test information.

The wavelet-aggregated signal used in this work allows to identify those regions in cervix where lesions are present, complementing our previous work and giving support to the approach presented before. The main advantage of wavelet analysis is that this technique supress local noise present in the curve obtained from temporal analysis, preserving just the variations corresponding to lesions in the cervix surface.

Texture metrics results showed a good correlation with the changes presented in the images. Results show to be promising because there are important differences between normal and abnormal cases using a set of medical cases.

Direction for future work is to use not just texture information but other parameters like three-dimensional data as well as use another basis function in wavelet analysis instead of just Haar function.

ACKNOWLEDGEMENTS

REFERENCES

Baeg S., Kehtarnavaz N., 2002. *Classification of Breast Mass Abnormalities using Denseness and Architectural Distortion,* Electronics Letters on Computer Vision and Image Analysis, Vol. 1 Num. 1 pp. 1-20.

Barreto F.A., Altamirano R.L., Morales T.R.M., Cisneros A.J.D., 2005. *Identifying Precursory Cancer Lesions Using Temporal Texture Analysis,* Second Canadian Conference on Computer and Robot Vision.

Burghardt E., 1991. *Colposcopy-Cervical Pathology*, Textbook and Atlas, Thieme Germany.

Claude I., Pouletaut P., Huault S., Boulanger J-C, 2001. *Integrated Color and Texture Tools for Colposcopy Image Segmentation*, International Conference Image Processing IEEE.

Claude I., Winzenrieth R., Pouletaut P., Boulanger J-C, 2002. *Contour Features for Colposcopic Image Classification by Artificial Neural Network*, 16 th International Conference on Pattern Recognition IEEE.

Lyubushin A.A., 1998. *An Aggregated Signal of the Low-Frequency Geophysical Monitoring Systems,* Fiz. Zemli Num. 3 pp. 69–74.

Lyubushin A.A., 2000. *Wavelet-Aggregated Signal and Synchronous Peaked Fluctuations in Problems of Geophysical Monitoring and Earthquake Prediction,* Fiz. Zemli Num. 3 pp. 20–30.

Parker M.F., Karins J.P., O´Connor D.M., 1998. *Hyperspectral Diagnostic Imaging of the Cervix: Initial Observations,* Proceedings of the Pacific Medical Technology Symposium IEEE.

Parker M.F., Mooradian G.C., Okimoto G.S., et al, 2002. *Initial Neural Net Construction for the Detection of Cervical Intraephithelial Neoplasia by Fluorescence Imaging,* American Journal of Obstetrics and Gynecology.

Pogue B.W., Mycek M.A., Harper D., 2000. *Image Analysis for Discrimination of Cervical Neoplasia,* Journal of Biomedical Optics SPIE, Vol. 5 pp.72–82.

Tapia L.D., Barreto F.A., Altamirano R.L., 2006. *Identifying cervical cancer lesions using temporal texture analysis,* Fourth IASTED International Conference on Biomedical Engineering, Innsbruck Austria.

Tumer K., Ramanujam N., Ghosh J., Kortum R.R., 1998. *Ensembles of Radial Basis Function Networks for Spectroscopy Detection of Cervical Precancer,* IEEE Transactions on Biomedical Engineering, Vol. 45 Num. 8. pp. 953-961.

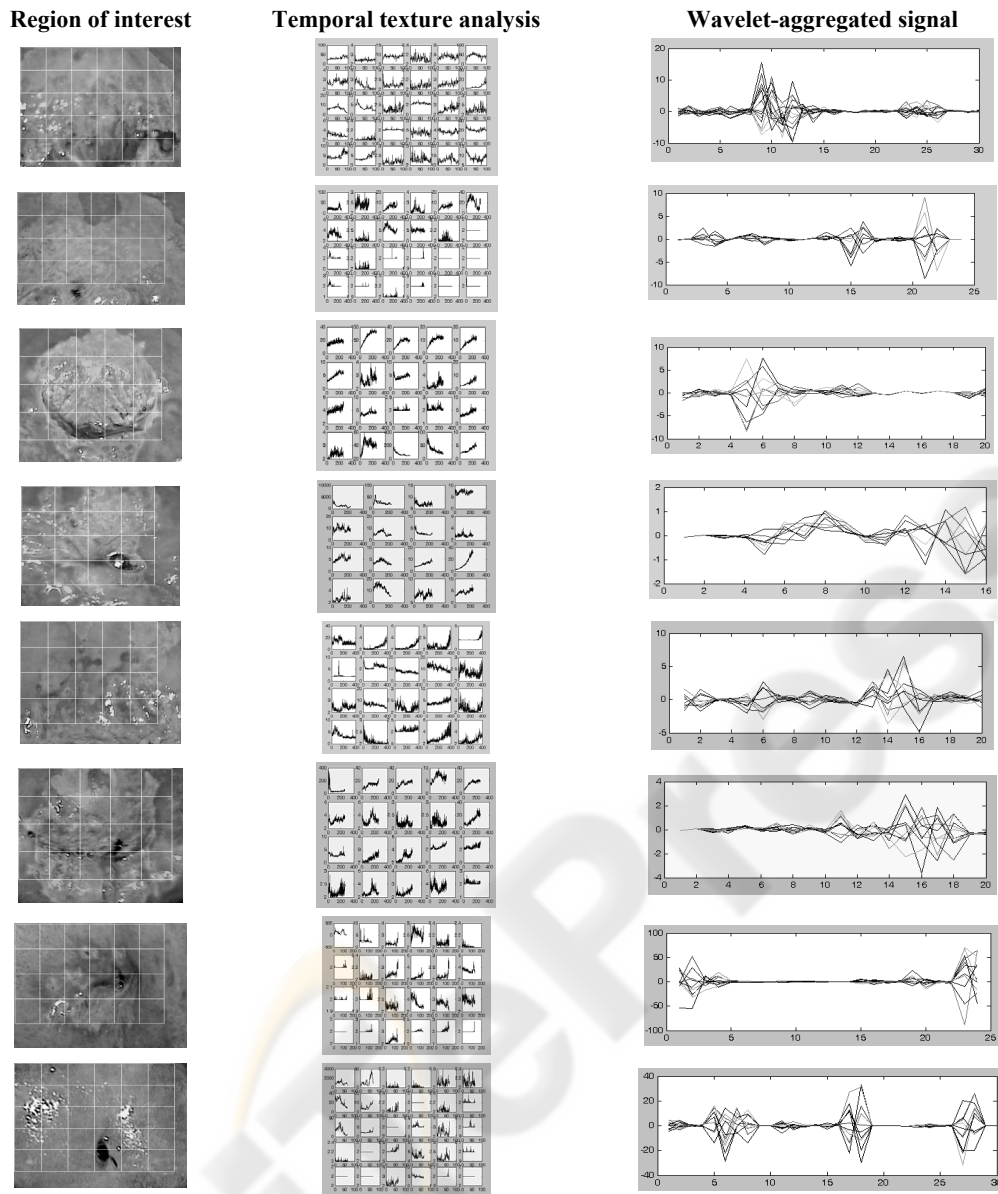| Region of interest	Temporal texture analysis	Wavelet-aggregated signal

Figure 4: Temporal information obtained with temporal texture analysis and wavelet-aggregated signal for every case.

Table 2: Classification results using several learning algorithms.

C	ALGORITHMS					
	1-NN		Naive Bayes		Backpropagation	
	Accuracy (%)	F-Measure (%)	Accuracy (%)	F-Measure (%)	Accuracy (%)	F-Measure (%)
1	73.33	77.8	73.33	77.8	73.33	77.8
2	75	85	83.33	88.9	75	85
3	75	83.9	73.684	81.5	70	81.3
4	56.25	72	62.5	70	43.75	60.9
5	50	61.5	70	76.9	30	34.8
6	65	78.8	80	84.6	80	87.5
7	75	85	87.5	90.9	75	85
8	70	80	83.33	87.2	80	87